Reduction or Enhancement of Stellarator Turbulence by Impurities

J. M. García-Regaña,[1,*] I. Calvo,[1] F. I. Parra,[2] and H. Thienpondt[1]
[1]*Laboratorio Nacional de Fusión, CIEMAT, 28040 Madrid, Spain*
[2]*Princeton Plasma Physics Laboratory, Princeton, New Jersey 08540, USA*

(Received 1 June 2023; revised 13 June 2024; accepted 22 July 2024; published 6 September 2024)

A systematic study of the impact of impurities on the turbulent heat fluxes is presented for the stellarator Wendelstein 7-X (W7-X) and, for comparison, the Large Helical Device and ITER. By means of nonlinear multispecies gyrokinetic simulations, it is shown that impurities, depending on the sign of their density gradient, can significantly enhance or reduce turbulent ion heat losses. For the relevant scenario of turbulence reduction, an optimal impurity concentration that minimizes the ion heat diffusivity emerges as a universal feature. This result demonstrates the potential of impurities for controlling turbulence and accessing enhanced confinement regimes in fusion plasmas and, in particular, in W7-X.

DOI: 10.1103/PhysRevLett.133.105101

The stellarator is a promising concept for magnetic confinement fusion reactors, mainly due to its intrinsic steady-state operation and absence of disruptions. Nonetheless, the actual possibility for the stellarator to become competitive against the tokamak has historically been handicapped by two main difficulties: the substantially larger neoclassical particle and heat losses caused by the three-dimensionality of the magnetic field, and the more challenging engineering and manufacturing required to build stellarators, compared to tokamaks. In relation to these two difficulties, Wendelstein 7-X (W7-X), the most advanced stellarator in operation, has represented a huge leap forward. First, W7-X has been optimized for reduced neoclassical transport by a careful tailoring of the magnetic configuration. The success of this optimization strategy has been demonstrated experimentally, leading to record values of the fusion triple product in stellarators [1]. Second, despite the complexity of the system of modular coils needed to produce the desired configuration, measured errors are smaller than one part in 100 000 [2], which meets the crucial milestone of building a large optimized stellarator within restrictive tolerances.

W7-X has also brought to the forefront other questions to which less importance has traditionally been given. Because of the successful reduction of neoclassical losses, turbulence has become, in general, the main transport channel. In standard ECRH W7-X plasmas, power balance analyses show that heat fluxes are predominantly turbulent throughout the entire plasma volume [3]. In those scenarios a stiff turbulent heat transport has been pointed out as the reason why the core ion temperature clamps at approximately 1.5 keV, which is considerably lower than the values predicted by neoclassical theory. So far, a higher core ion temperature has only been achieved in high performance scenarios with reduced turbulence, where the neoclassical optimization of W7-X has been experimentally confirmed [1]. Such scenarios have been transiently reached by means of series of cryogenic pellet injections, which increase the density gradient of the main species and moves the operation point from a region in the space of profile gradients where ion-temperature-gradient (ITG) turbulence is close to be maximal to a region where it is significantly attenuated. This mechanism for reducing turbulence has been confirmed by means of numerical simulations [4] and is demonstrated to be particularly efficient in W7-X, in comparison with other stellarator configurations [5]. Since steady state operation is one of the main advantages of the stellarator concept, as well as a central goal of the W7-X project, the identification of additional mechanisms that mitigate turbulent heat losses beyond a transient phase is, therefore, pressingly required. In this Letter, we report on the role of impurities as a highly efficient actuator on turbulence. In order to assess the universality of the effects found, the Large Helical Device (LHD, Japan) and ITER are also considered. We have found that impurities can reduce or enhance the turbulent fluctuations and associated ion heat transport. In the three devices, an optimal concentration is found that minimizes the ion heat flux. Moreover, among the three, only W7-X exhibits a remarkable reduction in electron heat transport, mirroring the trend observed for the ion heat flux with varying impurity content. This work emphasizes the great potential of injecting impurities and controlling its concentration toward improving the plasma performance.

*Contact author: jose.regana@ciemat.es

Moreover, it also warns about conditions where impurities increase the turbulent heat losses.

The results that follow are obtained by means of electrostatic collisionless nonlinear simulations performed in flux tube geometry with the gyrokinetic code `stella` [6], which has already been applied to W7-X transport studies in a number of previous works [5,7–11]. All simulations are performed at the radial position $r/a = 0.7$. Here, r is the flux surface label and a is the minor radius of the device. We assume that the plasma consists of hydrogen nuclei, electrons, and a single impurity species with densities n_i, n_e, and n_z, respectively, all with the same temperature T and normalized temperature gradient $a/L_T = 3.0$. Here, the normalized gradient of a physical quantity X is defined as $a/L_X = -a\mathrm{d}\ln X/\mathrm{d}r$. The equilibrium density of electrons and impurities as well as their normalized gradients are constrained by the lowest-order quasineutrality equation and its radial derivative. Namely,

$$n_e = n_i + Zn_z, \tag{1}$$

$$a/L_{n_e} = (n_i/n_e)a/L_{n_i} + (Zn_z/n_e)a/L_{n_z}, \tag{2}$$

with Z the charge state of the impurity. Throughout the present study, the main ion density, taken as reference value, and its density gradient ($a/L_{n_i} = 1.0$) have remained unchanged [12].

For W7-X, we have performed a scan of the impurity density gradient a/L_{n_z} in the range $[-6, 6]$ for C^{6+} and Fe^{16+} impurities at concentrations such that $Z_{\mathrm{eff}} = 1.4$, with $Z_{\mathrm{eff}} = \sum_j Z_j^2 n_j/n_e$ and j running over the ion species of the plasma. Figures 1(a) and 1(b) display, respectively, the ion (Q_i) and electron (Q_e) heat fluxes in gyro-Bohm units for these series of simulations. The electron heat flux is multiplied by n_i/n_e in order to balance out the Q_e increase due to the fact that $n_e/n_i > 1$ when $Z_{\mathrm{eff}} > 1$. In the first place, comparing the black and red curves of, respectively, Q_i and Q_e, with their values with no impurities, shown in gray, it can be clearly observed that both fluxes are modified by the presence of impurities. Roughly, Q_i and Q_e are enhanced when the impurity density is hollow and are reduced when the impurity density is peaked. Second, the impact of carbon is appreciably stronger than that of the heavier and more highly charged iron impurity.

Figure 2 shows, for LHD and ITER as well, Q_i and Q_e as a function of a/L_{n_z} considering C^{6+} as impurity. Although more moderate in these two devices, Q_i reduction (or enhancement) occurs when a/L_{n_z} is positive (or negative), as in W7-X. This dependence of Q_i on a/L_{n_z} strongly resembles the role that impurities have on the ITG stability in simplified geometries [27–30]. In those references, the linear growth rate increases or decreases depending on whether the main ions and impurities have, respectively, antiparallel or parallel density gradients. The results

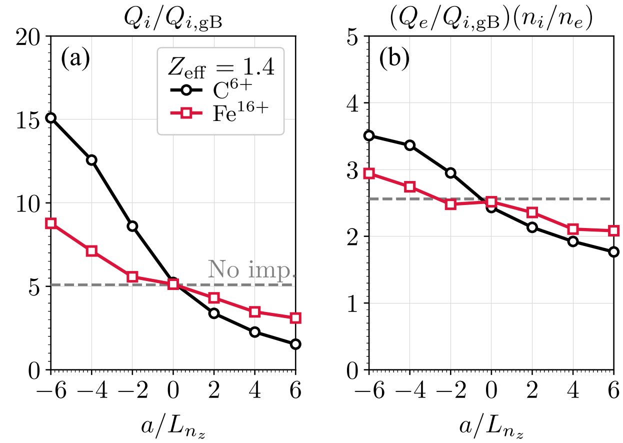

FIG. 1. Main ion (a) and electron (b) heat fluxes as a function of the impurity density gradient in W7-X, considering Fe^{16+} (squares) and C^{6+} (circles), each as a single impurity in a plasma with $Z_{\mathrm{eff}} = 1.4$. For all the figures of the Letter, quantities have been averaged over time during the saturated phase. In addition, heat fluxes are normalized to the ion gyro-Bohm value [12], and heat flux levels in the absence of impurities are indicated by the dashed gray line.

discussed so far in this Letter demonstrate that the ion heat reduction or enhancement holds for nonlinear turbulence, regardless of the magnetic geometry, and when all species are treated kinetically. In contrast, the effect on Q_e is clearly less pronounced and the trend is different from one device to another: for LHD, Q_e is practically independent on a/L_{n_z}; for ITER, Q_e increases with increasing a/L_{n_z}, transitioning from a slight reduction to enhancement; and only W7-X exhibits a similar behavior for Q_e as for Q_i.

It must be emphasized that, when impurities are included in these simulations, the only bulk plasma parameters

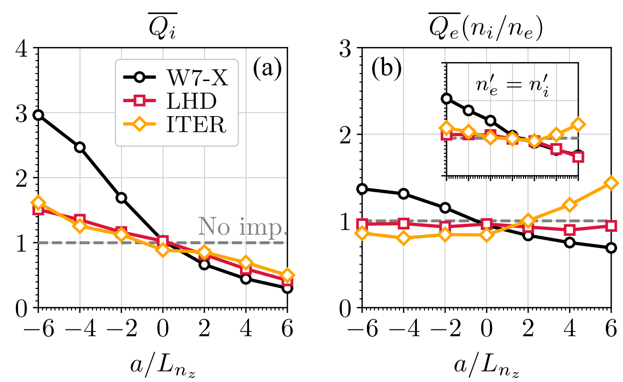

FIG. 2. Main ion (a) and electron (b) heat fluxes as a function of the impurity density gradient, considering C^{6+} and $Z_{\mathrm{eff}} = 1.4$ for W7-X, LHD, and ITER. The inset shows the inconsistent case where $a/L_{n_i} = a/L_{n_e}$ (see main text). Throughout this work, an overbar denotes normalization of the quantity with respect to its value in the absence of impurities.

modified are the electron density and its gradient, consistently with Eqs. (1) and (2) (in the scan along a/L_{n_z} from −6 to 6, a/L_{n_e} has been modified from 0.4 to 1.4). Since a/L_{n_e} is a free energy source for the electrons, one might wonder whether the differences in Q_e are due to the sole presence of the impurity or due to the different impact each configuration might experience to the modification of a/L_{n_e}. To investigate this, we have performed simulations inconsistent with Eq. (2), forcing $a/L_{n_e} = a/L_{n_i}$, despite the presence of the impurity. The results, depicted in the inset of Fig. 2(b), allow us to conclude that Q_e in different configurations shows different trends mostly due to the sole presence of the impurity, and not due to a/L_{n_e}. This conclusion does not change qualitatively when compared with the data in the main figure. Nevertheless, a correction due to the modification of a/L_{n_e}, that we explore further below, can be inferred.

Beyond heat fluxes, the amplitude of the electrostatic potential fluctuations is, analogously to Q_i, enhanced or reduced, as Fig. 3(a) shows for the case with C^{6+} and the three analyzed devices. Figures 3(b) and 3(c) depict the ratio of, respectively, the ion and electron heat fluxes over the squared electrostatic fluctuations $\langle\varphi^2\rangle$, where $\langle\ldots\rangle$ denotes the average over the flux tube volume. For ions, $Q_i/\langle\varphi^2\rangle$ depends weakly on a/L_{n_z}, which indicates that the ion heat flux is strongly tied to the fluctuation level of the potential. In other words, the ion heat flux decreases or increases as turbulent fluctuations do. In contrast, Fig. 3(c) shows that Q_e increases more sharply with a/L_{n_z} than $\langle\varphi^2\rangle$ does. Remarkably, all devices exhibit a similar trend, which roughly follows that of a/L_{n_e}, depicted for clarity. As a/L_{n_e} is equally increased in all three devices, the alignment is not surprising. This indicates that, ultimately, despite the different impact that the presence of the impurity alone has on Q_e for each device [see inset of Fig. 2(b)], the correction due to a/L_{n_e} is comparable for all three devices, at least in this case of a moderate Z_{eff} of 1.4.

With regard to the case of turbulence reduction, it is then natural to wonder how large the impurity concentration must be in order to maximize heat flux reduction (impurity-induced reduction of turbulence in tokamak [31] and stellarator [22,32–34] experiments is moderately reported, and simulations have occasionally pointed out to this impurity effect in tokamak geometry [35,36]). To answer this question, a scan in the effective charge has been performed for the case of C^{6+} with $a/L_{n_z} = 6$. For W7-X, the results for the main ion and impurity heat fluxes are represented in Fig. 4(a) and for the electron heat flux in Fig. 4(b). Both Q_i and Q_e decrease with growing effective charge up to the value $Z_{\mathrm{eff}} = 2$. The decrease is more significant for Q_i, which is reduced by an order of magnitude, than for Q_e, which is halved. In contrast, for $Z_{\mathrm{eff}} > 2$ both Q_i and Q_e grow with Z_{eff}. In the range from $Z_{\mathrm{eff}} \approx 2$ to $Z_{\mathrm{eff}} \approx 3$, Q_i recovers approximately one third of its value in the absence of impurities, whereas Q_e enhances its level clearly above that without impurities. This increasing trend is due to the increasing value of a/L_{n_e} imposed by Eq. (2). Ignoring Eq. (2), i.e., forcing $a/L_{n_e} = a/L_{n_i}$ (dashed lines), makes Q_e and Q_i decrease mononotically with Z_{eff} in the entire represented range. Furthermore, the impurity heat flux consistently remains low and does not counterbalance the decrease in the heat flux of the main species. Similar Z_{eff} scans for LHD and ITER, depicted in Fig. 5, reveal the local minimum of Q_i as a universal feature, occurring at a value of $Z_{\mathrm{eff}} \sim 1.5$–2.0. On the other hand, the impurity heat flux increases strongly with Z_{eff}, and the electron heat flux is not decreased with increasing Z_{eff}, in contrast to W7-X. However, the idea of an optimal concentration for overall reduction of turbulence holds. For instance, at $Z_{\mathrm{eff}} \sim 1.75$ in LHD, Q_i is minimum, and neither Q_e nor $Q_{C^{6+}}$ have increased much—interestingly,

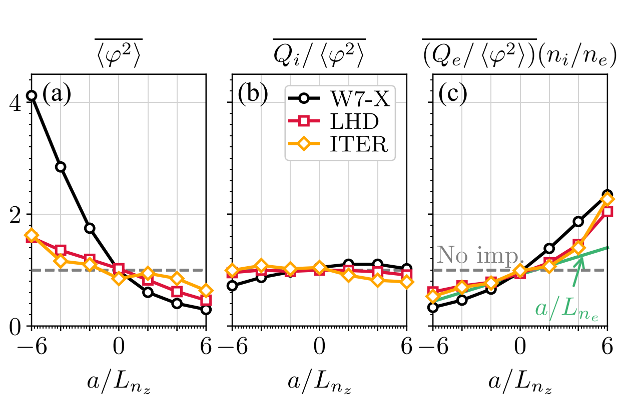

FIG. 3. For C^{6+} impurities at a concentration such that $Z_{\mathrm{eff}} = 1.4$: dependence on the impurity density gradient of (a) the averaged squared potential fluctuations, $\langle\varphi^2\rangle$, and (b) the main ion and (c) electron heat fluxes over $\langle\varphi^2\rangle$ for W7-X, LHD and ITER. For clarity, a/L_{n_e} is illustrated in (c).

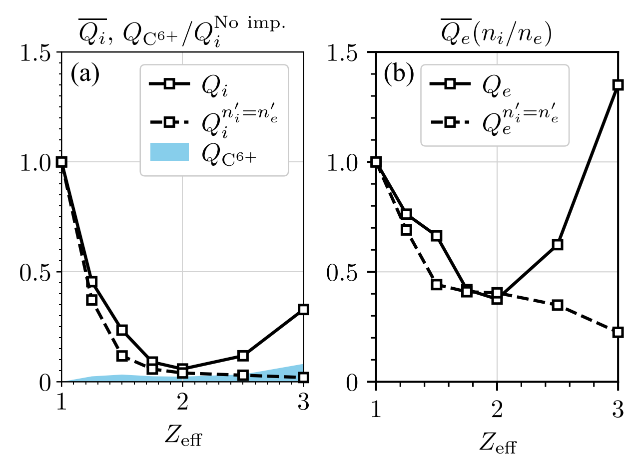

FIG. 4. For W7-X, heat fluxes of (a) main and impurity ions, and (b) electrons as a function of Z_{eff}, with C^{6+} the only impurity present in the plasma.

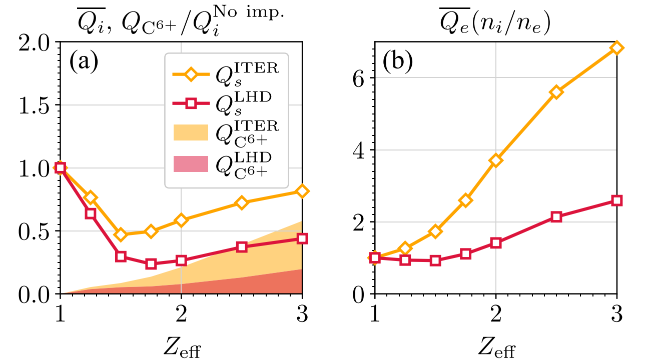

FIG. 5. For LHD and ITER, heat fluxes of (a) main and impurity ions, and (b) electrons as a function of Z_{eff}, with C^{6+} the only impurity present in the plasma.

carbon injections have traditionally assisted in accessing high-T_i plasmas with internal transport barriers in LHD [22], and the dependence of ion heat diffusivity on carbon concentration, with an evident resemblance to our $Q_i(Z_{\text{eff}})$ curve, has been reported in [32].

Returning to the evidently interesting case of W7-X, the reason why Q_e is not reduced as much as Q_i in the range from $Z_{\text{eff}} = 1$ up to 2, and why it increases more significantly than Q_i beyond that range is likely due to the transition to an electron-density-gradient-driven dominated turbulence, as is shown next. Let $(\delta n_s)^2(\theta)$ be the squared density fluctuations of species s as a function of the poloidal coordinate, and $(\delta n)^2_{\text{max}} = \max\{\delta n_i^2(\theta), \delta n_e^2(\theta), \delta n_z^2(\theta), \theta \in [-\pi, \pi]\}$ the largest density fluctuation amplitude found along θ. Figures 6(a)–6(e) show, for $Z_{\text{eff}} = \{1.0, 1.5, 2.0, 2.5, 3.0\}$, $(\delta n_s)^2(\theta)/(\delta n)^2_{\text{max}}$ for the main ions, electrons, and C^{6+}. The squared electrostatic potential fluctuations as a function of the poloidal angle, $\varphi^2(\theta)$, normalized to its maximum value, $\varphi^2_{\text{max}} = \max\{\varphi^2(\theta), \theta \in [-\pi, \pi]\}$, is also represented. Examining this figure, it can be observed how the increase of Z_{eff} modifies the turbulent electrostatic potential, from strongly localized at the center to becoming spread out along the flux tube. Moreover, the main ion density fluctuations become significantly reduced with respect to those of the electrons, particularly for $Z_{\text{eff}} = \{2.5, 3.0\}$. For these high impurity concentration cases, $\delta n_e^2(\theta)$ coincides almost exactly with $Z^2 \delta n_z^2(\theta)$, pointing out that the main ions do not respond to the turbulence. In addition, electron density fluctuations are strongly localized in the regions of magnetic field wells [see Fig. 6(f) for the magnetic field strength, B, as a function of θ]. This indicates that, as Z_{eff} and, consequently, a/L_{n_e} increase, turbulence acquires a vigorous TEM character, as we anticipated above. Such a change in the turbulence characteristics explains why the electron heat flux increases abruptly for $Z_{\text{eff}} > 2$ while the ion heat flux is not affected to the same extent in Fig. 4.

In summary, in this Letter we have presented the first systematic numerical study of the effect of impurities on bulk turbulence in W7-X and, for comparison, in LHD and ITER. By means of nonlinear gyrokinetic simulations, we have demonstrated that impurities can effectively alter turbulent heat transport. This finding is robust and

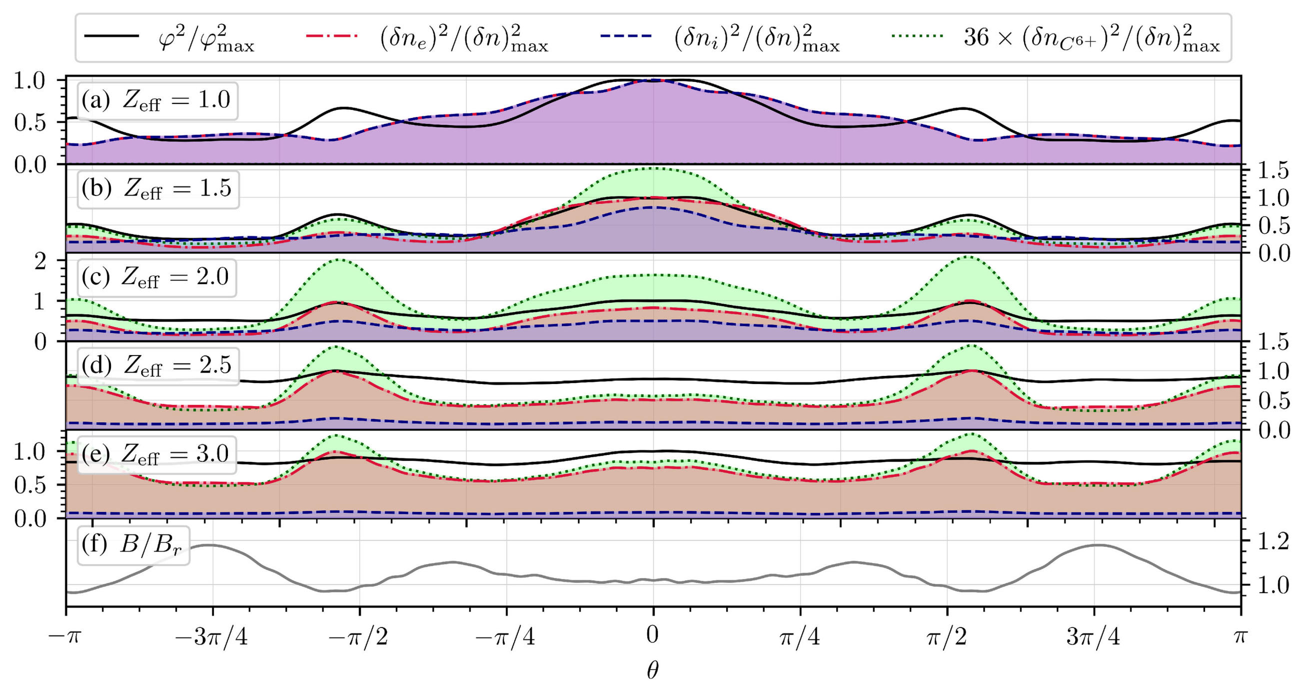

FIG. 6. For the Z_{eff} scan depicted in Fig. 4: (a)–(e) shows the normalized electrostatic potential fluctuations, $\varphi^2/\varphi^2_{\text{max}}$, and normalized density fluctuations, $(\delta n_s)^2/(\delta n)^2_{\text{max}}$, of main ions, electrons, and C^{6+} as a function of the poloidal coordinate; (f) shows the modulus of the magnetic field.

manifests both for electron and, more substantially, ion heat fluxes in the three configurations. This has obvious interest for future reactors, as the main ions are the reactants in the fusion fuel. When the density gradient of impurities and main species are, roughly, parallel (respectively, antiparallel), turbulent fluctuations and ion heat losses decrease (respectively, increase). As for the electron heat flux, the combination of the impurity effect and the response of the configuration to modifications of a/L_{n_e} forced by quasineutrality, introduces differences across the devices, which will be thoroughly addressed in upcoming studies. A central message of the present work is that, regardless of the magnetic configuration, the ion heat flux reaches a minimum value at a specific impurity concentration, that could be seen as an optimal impurity content to operate with as long as radiative losses were tolerable. As a particularly interesting case, in W7-X, when Q_i is reduced, Q_e is also reduced and the impurity heat flux remains low. In summary, the present study emphasizes the ambivalent role of impurities and their potential to enhance or degrade the performance of magnetically confined plasmas through its active role on turbulence.

Acknowledgments—J. M. G. R. is grateful to Michael Barnes for his support with the code `stella` and to Arturo Alonso and Felix Reimold for fruitful discussions. This work has been carried out within the framework of the EUROfusion Consortium, funded by the European Union via the Euratom Research and Training Programme (Grant Agreement No. 101052200–EUROfusion). This research was supported in part by Grant No. PID2021-123175NB-I00, Ministerio de Ciencia e Innovación, Spain. This work was supported by the U.S. Department of Energy under Contract No. DE-AC02-09CH11466. Simulations were performed in the supercomputers Marconi (CINECA, Italy) and Marenostrum (Barcelona Supercomputing Center, Spain).

[1] C. D. Beidler, H. M. Smith, A. Alonso, T. Andreeva, J. Baldzuhn, M. N. A. Beurskens, M. Borchardt, S. A. Bozhenkov, K. J. Brunner, H. Damm *et al.*, Demonstration of reduced neoclassical energy transport in Wendelstein 7-X, Nature (London) **596**, 221 (2021).

[2] T. Sunn Pedersen, M. Otte, S. Lazerson, P. Helander, S. Bozhenkov, C. Biedermann, T. Klinger, R. C. Wolf, and H.-S. Bosch (The Wendelstein 7-X Team), Confirmation of the topology of the Wendelstein 7-X magnetic field to better than 1:100,000, Nat. Commun. **7**, 13493 (2016).

[3] S. A. Bozhenkov, Y. Kazakov, O. P. Ford, M. N. A. Beurskens, J. Alcusón, J. A. Alonso, J. Baldzuhn, C. Brandt, K. J. Brunner, H. Damm *et al.*, High-performance plasmas after pellet injections in Wendelstein 7-X, Nucl. Fusion **60**, 066011 (2020).

[4] P. Xanthopoulos, S. A. Bozhenkov, M. N. Beurskens, H. M. Smith, G. G. Plunk, P. Helander, C. D. Beidler, J. A. Alcusón, A. Alonso, A. Dinklage *et al.*, Turbulence mechanisms of enhanced performance stellarator plasmas, Phys. Rev. Lett. **125**, 075001 (2020).

[5] H. Thienpondt, J. M. García-Regaña, I. Calvo, G. Acton, and M. Barnes, Influence of the density gradient on turbulent heat transport at ion-scales: An inter-machine study with the gyrokinetic code `stella`, arXiv:2404.09929 [Nucl. Fusion (to be published)].

[6] M. Barnes, F. I. Parra, and M. Landreman, `stella`: An operator-split, implicit-explicit δf-gyrokinetic code for general magnetic field configurations, J. Comput. Phys. **391**, 365 (2019).

[7] J. M. García-Regaña, M. Barnes, I. Calvo, F. I. Parra, J. A. Alcusón, R. Davies, A. González-Jerez, A. Mollén, E. Sánchez, J. L. Velasco, and A. Zocco, Turbulent impurity transport simulations in Wendelstein 7-X plasmas, J. Plasma Phys. **87**, 855870103 (2021).

[8] J. M. García-Regaña, M. Barnes, I. Calvo, A. González-Jerez, H. Thienpondt, E. Sánchez, F. I. Parra, and D. A. St.-Onge, Turbulent transport of impurities in 3D devices, Nucl. Fusion **61**, 116019 (2021).

[9] H. Thienpondt, J. M. García-Regaña, I. Calvo, J. A. Alonso, J. L. Velasco, A. González-Jerez, M. Barnes, K. Brunner, O. Ford, G. Fuchert *et al.*, Prevention of core particle depletion in stellarators by turbulence, Phys. Rev. Res. **5**, L022053 (2023).

[10] A. Zocco, L. Podavini, J. M. García-Regaña, M. Barnes, F. I. Parra, A. Mishchenko, and P. Helander, Gyrokinetic electrostatic turbulence close to marginality in the Wendelstein 7-X stellarator, Phys. Rev. E **106**, L013202 (2022).

[11] L. Podavini, A. Zocco, J. M. García-Regaña, M. Barnes, F. I. Parra, A. Mishchenko, and P. Helander, Electrostatic microinstabilities and turbulence in Wendelstein 7-X close to the stability threshold, arXiv:2311.04342 [J. Plasma Phys. (to be published)].

[12] See Supplemental Material at http://link.aps.org/supplemental/10.1103/PhysRevLett.133.105101, which includes Refs. [13–26], for details on the normalization conventions, choice of plasma parameters, magnetic configurations and convergence of the numerical simulations.

[13] C. Kessel, G. Giruzzi, A. Sips, R. Budny, J. Artaud, V. Basiuk, F. Imbeaux, E. Joffrin, M. Schneider, M. Murakami *et al.*, Simulation of the hybrid and steady state advanced operating modes in ITER, Nucl. Fusion **47**, 1274 (2007).

[14] D. Campbell, The first fusion reactor: ITER, Europhys. News **47**, 28 (2016).

[15] S. P. Hirshman and J. C. Whitson, Steepest-descent moment method for three-dimensional magnetohydrodynamic equilibria, Phys. Fluids **26**, 3553 (1983).

[16] R. L. Miller, M. S. Chu, J. M. Greene, Y. R. Lin-Liu, and R. E. Waltz, Noncircular, finite aspect ratio, local equilibrium model, Phys. Plasmas **5**, 973 (1998).

[17] J.-P. Bähner, J. Alcusón, S. Hansen, A. von Stechow, O. Grulke, T. Windisch, H. Smith, Z. Huang, E. Edlund, M. Porkolab *et al.*, Phase contrast imaging measurements and numerical simulations of turbulent density fluctuations in gas-fuelled ECRH discharges in Wendelstein 7-X, J. Plasma Phys. **87**, 905870314 (2021).

[18] T. Estrada, D. Carralero, T. Windisch, E. Sánchez, J. M. García-Regaña, J. Martínez-Fernández, A. de la Peña, J. L. Velasco, J. A. Alonso, M. Beurskens *et al.*, Radial electric field and density fluctuations measured by Doppler reflectometry during the post-pellet enhanced confinement phase in W7-X, Nucl. Fusion **61**, 046008 (2021).

[19] A. Bañón Navarro, G. Merlo, G. G. Plunk, P. Xanthopoulos, A. von Stechow, A. Di Siena, M. Maurer, F. Hindenlang, F. Wilms, and F. Jenko, Global gyrokinetic simulations of ITG turbulence in the magnetic configuration space of the Wendelstein 7-X stellarator, Plasma Phys. Controlled Fusion **62**, 105005 (2020).

[20] A. González-Jerez, J. M. García-Regaña, I. Calvo, D. Carralero, T. Estrada, E. Sanchez, and M. Barnes, Electrostatic microturbulence in W7-X: Comparison of local gyrokinetic simulations with Doppler reflectometry measurements, Nucl. Fusion **64**, 076029 (2024).

[21] D. Carralero, T. Estrada, E. Maragkoudakis, T. Windisch, J. A. Alonso, M. Beurskens, S. Bozhenkov, I. Calvo, H. Damm, O. Ford, G. Fuchert, J. M. García-Regaña, N. Pablant, E. Sánchez, E. Pasch, and J. L. Velasco (The Wendelstein 7-X Team), An experimental characterization of core turbulence regimes in Wendelstein 7-X, Nucl. Fusion **61**, 096015 (2021).

[22] H. Takahashi, K. Nagaoka, K. Mukai, M. Yokoyama, S. Murakami, S. Ohdachi, T. Bando, Y. Narushima, H. Nakano, M.Osakabe *et al.*, Realization of high T_i plasmas and confinement characteristics of ITB plasmas in the LHD deuterium experiments, Nucl. Fusion **58**, 106028 (2018).

[23] Y. Nakamura, N. Tamura, M. Kobayashi, S. Yoshimura, C. Suzuki, M. Yoshinuma, M. Goto, G. Motojima, K. Nagaoka, K. Tanaka *et al.*, A comprehensive study on impurity behavior in LHD long pulse discharges, Nucl. Mater. Energy **12**, 124 (2017).

[24] A. Langenberg, T. Wegner, O. Marchuk, J. M. García-Regaña, N. Pablant, G. Fuchert, S. Bozhenkov, H. Damm, E. Pasch, K.-J. Brunner *et al.*, Impurity transport in ion- and electron-root confinement scenarios at Wendelstein 7-X, Nucl. Fusion **61**, 116018 (2021).

[25] T. Romba, F. Reimold, R. Jaspers, O. Ford, L. Vanó, and T. Klinger, Suppression of anomalous impurity transport in NBI-heated W7-X plasmas, Nucl. Fusion **63**, 076023 (2023).

[26] A. González-Jerez, P. Xanthopoulos, J. M. García-Regaña, I. Calvo, J. Alcusón, A. Bañón Navarro, M. Barnes, F. I. Parra, and J. Geiger, Electrostatic gyrokinetic simulations in Wendelstein 7-X geometry: Benchmark between the codes `stella` and GENE, J. Plasma Phys. **88**, 905880310 (2022).

[27] W. M. Tang, R. B. White, and P. N. Guzdar, Impurity effects on ion-drift-wave eigenmodes in a sheared magnetic field, Phys. Fluids **23**, 167 (1980).

[28] R. Dominguez and G. Staebler, Impurity effects on drift wave stability and impurity transport, Nucl. Fusion **33**, 51 (1993).

[29] J. Q. Dong, W. Horton, and W. Dorland, Isotope scaling and η_i mode with impurities in tokamak plasmas, Phys. Plasmas **1**, 3635 (1994).

[30] J. Q. Dong and W. Horton, Studies of impurity mode and ion temperature gradient mode in toroidal plasmas, Phys. Plasmas **2**, 3412 (1995).

[31] G. McKee, K. Burrell, R. Fonck, G. Jackson, M. Murakami, G. Staebler, D. Thomas, and P. West, Impurity-induced suppression of core turbulence and transport in the DIII-D tokamak, Phys. Rev. Lett. **84**, 1922 (2000).

[32] M. Osakabe, H. Takahashi, K. Nagaoka, S. Murakami, I. Yamada, M. Yoshinuma, K. Ida, M. Yokoyama, R. Seki, H. Lee *et al.*, Impact of carbon impurities on the confinement of high-ion-temperature discharges in the Large Helical Device, Plasma Phys. Controlled Fusion **56**, 095011 (2014).

[33] F. Nespoli, S. Masuzaki, K. Tanaka, N. Ashikawa, M. Shoji, E. P. Gilson, R. Lunsford, T. Oishi, K. Ida, M. Yoshinuma *et al.*, Observation of a reduced-turbulence regime with boron powder injection in a stellarator, Nat. Phys. **18**, 350 (2022).

[34] R. Lunsford, C. Killer, A. Nagy, D. A. Gates, T. Klinger, A. Dinklage, G. Satheeswaran, G. Kocsis, S. A. Lazerson, F. Nespoli *et al.*, Characterization of injection and confinement improvement through impurity induced profile modifications on the Wendelstein 7-X stellarator, Phys. Plasmas **28**, 082506 (2021).

[35] I. Pusztai, J. Candy, and P. Gohil, Isotope mass and charge effects in tokamak plasmas, Phys. Plasmas **18**, 122501 (2011).

[36] X. Wei, H. Yang, and S. Li, Y. Xiao, Gyrokinetic particle simulation of electrostatic microturbulence with impurity ions, Phys. Plasmas **25**, 082508 (2018).